New searches for the C-noninvariant decay $\pi^0 \to 3\gamma$ and the rare decay $\pi^0 \to 4\gamma$

J. McDonough,* V. L. Highland, and W. K. McFarlane
Temple University, Philadelphia, Pennsylvania 19122

R. D. Bolton, M. D. Cooper, J. S. Frank,† A. L. Hallin,‡ P. Heusi,§ C. M. Hoffman, G. E. Hogan, F. G. Mariam, R. E. Mischke, L. E. Piilonen,** V. D. Sandberg, U. Sennhauser,†† R. D. Werbeck, R. A. Williams, and S. L. Wilson
Los Alamos National Laboratory, Los Alamos, New Mexico 87545

D. P. Grosnick‡‡ and S. C. Wright
University of Chicago, Chicago, Illinois 60637
(Received 26 May 1988)

A search for the charge-conjugation-noninvariant decay $\pi^0 \to 3\gamma$ has been made using the Crystal Box of the Los Alamos Meson Physics Facility. No signal in excess of background was observed, resulting in a branching-ratio upper limit of 3.1×10^{-8} (90% C.L.). A new upper limit of 2×10^{-8} (90% C.L.) was also established for the allowed decay $\pi^0 \to 4\gamma$.

I. INTRODUCTION

We report here the results of a new search for the charge-conjugation-noninvariant decay $\pi^0 \to 3\gamma$. The operation of charge conjugation C reverses the sign of all the generalized charges of a system—electric charge, baryon number, lepton number, etc.—effectively replacing each particle by its antiparticle. The implications of C invariance for the decays of neutral systems were first explored systematically by Wolfenstein and Ravenhall.[1] Noting that detailed model calculations consistently gave a vanishing rate for the decay of a neutral spin-zero boson into three photons, they inferred that a general selection rule was at work, which they proceeded to formulate. Invariance of the standard electromagnetic interaction under C implies that photons are eigenstates of C with eigenvalue -1. If an interaction is invariant under C, there are consequent restrictions on the photon states that can result, so that a spin-zero system can decay into three photons or into two photons, but not into both. Early experiments confirmed these expectations for ortho- and parapositronium[2] and for the π^0, which was found to decay into two photons but not three. The branching ratio $b_{3\gamma}=\Gamma(\pi^0\to3\gamma)/\Gamma(\pi^0\to2\gamma)$ was measured[3] to be less than 1.2%.

The discovery[4] that, contrary to expectations, the weak interaction is invariant neither under parity inversion P nor under C led to a general reexamination of invariance principles. Bernstein and Michel[5] pointed out that there was actually very little empirical information bearing on the C, P, or T invariance properties of the π^0 and suggested several experiments. Cline and Dowd[6] then made a new search for the $\pi^0 \to 3\gamma$ decay, setting a limit on the branching ratio $b_{3\gamma} < 3.8\times10^{-4}$.

After the further discovery[7] of CP noninvariance in the weak interactions, the evidence concerning C invariance was critically examined once again. Bernstein, Feinberg, and Lee,[8] arguing that C noninvariance in the electromagnetic interaction of hadrons could provide a natural explanation of the magnitude of the observed CP violation, noted that the evidence concerning C invariance in these interactions was much weaker than usually supposed. For instance, conservation of electromagnetic current and C invariance of the strong interaction together prohibit C-noninvariant photonuclear processes. They further showed that the electromagnetic decays of many neutral systems are forbidden or inhibited by principles other than C invariance. In the case of the π^0 they estimated the maximum theoretically expected value of $b_{3\gamma}$ as 3×10^{-6}, taking into account the electromagnetic coupling, the available phase space, and momentum-dependent "centrifugal barrier" terms. Other estimates by Berends,[9] Weisberg,[10] Galfi and Marx,[11] and Tarasov[12] ranged from 10^{-6} to 10^{-9}. Estimates were also given for C-noninvariant branching ratios and decay asymmetries of the η^0 and other particles.

Several experiments were done to check these ideas, particularly in η^0 decays,[13] but no violation of C invariance was found. For the π^0 the upper limit on $b_{3\gamma}$ was reported[14] as 5×10^{-6} (90% C.L.). More recently this limit has been lowered[15] to 1.5×10^{-6} and then[16] to 3.7×10^{-7}.

C invariance is now embedded in the extremely successful "standard model" of particle interactions,[17] so that there are no current predictions of C-noninvariant reactions outside the weak interaction.[18] CP violation nevertheless remains an unsolved problem, and there are still relatively few experiments testing C invariance. Furthermore, in the absence of a theory that incorporates C noninvariance, there is no clear interpretation of limits found in one experiment, such as η^0 decay, in terms of another experiment, such as $\pi^0 \to 3\gamma$ decay. Although a succession of null experiments in various areas lends considerable credibility to the presumption of C invariance,

one cannot be certain that a given suppression is not dynamical in origin or that it is not due to some other selection rule. Because C invariance is a principle of fundamental interest, it is important to test it whenever the means to improve the experiments become available.

In any experiment to search for $\pi^0 \rightarrow 3\gamma$, the allowed decay $\pi^0 \rightarrow 4\gamma$ is a potential background. The experimental limit[19] on the branching ratio for this decay mode is $b_{4\gamma} < 1.6 \times 10^{-6}$ (90% C.L.); theoretical estimates[12,20] of $b_{4\gamma}$ have ranged from 10^{-9} to 10^{-16}. A by-product of this experiment is an improved experimental limit on $b_{4\gamma}$.

II. EXPERIMENTAL METHOD

The basic idea of the experiment was to produce π^0's by charge exchange of π^-'s at rest and then to search for the $\pi^0 \rightarrow 3\gamma$ decay using a large array of NaI crystals (Fig. 1). To obtain a significant yield of π^0's the π^-'s must be stopped in liquid hydrogen, in which the only significant reactions are $\pi^- p \rightarrow \pi^0 n$ and radiative capture $\pi^- p \rightarrow \gamma n$ in the proportion[21] 1.55:1. The π^0 has 27.9-MeV/c recoil momentum (137.8-MeV total energy), so that the photons from $\pi^0 \rightarrow 2\gamma$ decay are noncollinear by as much as 23° and have a uniform energy spectrum between 55 and 83 MeV. This decay mode was the source of the most significant backgrounds for the experiment, but it also furnished data for time and energy calibrations of the detector and provided a monitor of the total π^0 yield. The 129.4-MeV photon from radiative capture served as a high-energy calibration point for the detector, and $\pi^0 \rightarrow \gamma e^+ e^-$ provided a check of the time response at energies down to 12 MeV. Despite being a three-body electromagnetic decay, $\pi^0 \rightarrow \gamma e^+ e^-$ was not a significant background.

The experiment[22] was done in the Stopped Muon Channel at the Los Alamos Meson Physics Facility (LAMPF). A beam of 157-MeV/c negative pions, electrons, and muons in the proportions 3:3:1 was focused to a $\sim$3-cm-diameter spot with a momentum spread of approximately 6% [full width at half maximum (FWHM)]. These values, together with the energy straggling and multiple scattering inherent in degrading the energy of the beam pions to zero, determined the design of the hydrogen flask, which was a 10-mil Mylar cylinder 20 cm long $\times$ 10 cm in diameter having hemispherical end caps (Fig. 2). Scintillation counters S_1, S_2 (both $10 \times 10 \times 1.27$ cm), and S_3 (10 cm diameter $\times$ 0.3 cm thick) defined the beam. Pions came to rest in the hydrogen after passing through the beam counters, two beryllium degraders (8.1 and 5.8 g/cm^2), the 0.13-g/cm^2 Lexan vacuum window, and a 5.8-g/cm^2 graphite degrader. To reduce the transverse spread of the beam due to multiple scattering, the beam-counter/degrader system was made as compact as possible. The final graphite degrader was placed inside the vacuum chamber in contact with the hydrogen flask. Counter S_3 was placed just upstream of the flask and graphite. Approximately 75% of the π^-'s stopped in the hydrogen; the fraction that did not stop in the target was primarily due to multiple scattering rather than to range straggling. Muons and electrons passed through the flask and continued downstream beyond the detector.

Data were taken with a duty factor of 6.2% at average incident pion rates of 20, 40, and 50 kHz, with the majority at the intermediate rate. Three coincident photons readily occurred whenever more than one π^0 was produced by multiple π^-'s entering the target at the same time. Accordingly, the beam telescope logic rejected any event with a pulse height in S_2 larger than that corresponding to a single π^-. The final results showed no sensitivity to the beam intensity, but at higher rates accidental triggers became excessive and the NaI energy resolution was degraded.

A cylindrical scintillation counter 15 cm inner diameter, 1 cm thick, and 60 cm long surrounded the target flask. Twisted-strip light guides conducted the scintilla-

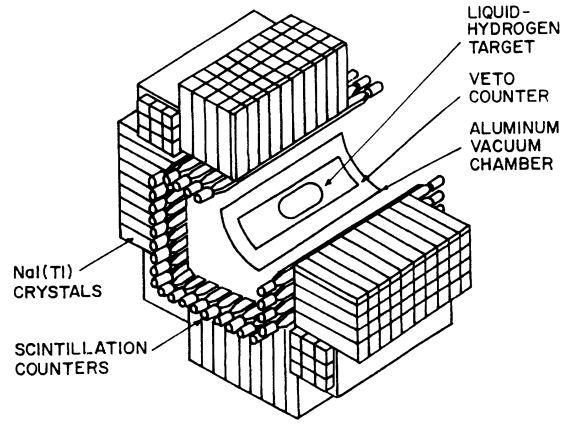

FIG. 1. Schematic view of the detector, omitting the beam counters.

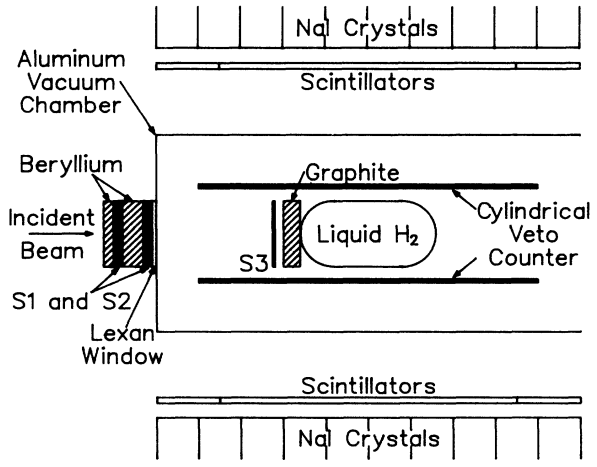

FIG. 2. Plan view of the beam telescope, hydrogen flask, and cylindrical veto counter.

tion light to two photomultipliers residing inside the vacuum chamber but receiving their dynode voltages from external dividers. The purpose of this counter was to identify electrons and positrons leaving the hydrogen before they could interact to produce photons. The target vacuum chamber was a cylinder of 2.3-mm aluminum with all its flanges and supports outside the detector volume.

The NaI detector array, the LAMPF Crystal Box, was originally designed for rare muon-decay experiments and has been described extensively elsewhere.[22–27] Briefly, it consisted of thallium-activated NaI crystals arranged as a four-sided hollow box (Fig. 1), which subtended a solid angle of approximately 2π sr about its center. Crystals measuring $6.35 \times 6.35 \times 30.5$ cm were organized both physically and electronically into four quadrants of nine rows (parallel to the beam) by ten columns. An additional 36 long crystals filled in the four corners between quadrants. To distinguish electrons from photons an array of scintillation counters $44.5 \times 5.7 \times 1.27$ cm covered the rows of NaI, except for the outer one and one-half columns at each end. Four additional scintillators on each face covered these outer columns, an arrangement required by the muon-decay experiments.

The yield of π^0's in the target was measured using an array of six crystals in the central two columns and three rows of each quadrant. The number of $\pi^0 \to 2\gamma$ coincidences between the arrays in opposite quadrants of the box was counted. These small arrays had modest counting rates with insignificant accidental rates and deadtimes. The appropriate thickness of beryllium degrader was set by maximizing the coincidence rate per incident beam particle. Using this monitor and a Monte Carlo calculation of its coincidence rate per π^0 decay, we find the total number of π^0's produced during the experiment to be $N_{\pi^0} = (1.75 \pm 0.05) \times 10^{10}$.

In the electronic logic used to select candidate events the NaI crystals in each row were organized into units by a logical OR of their (constant-fraction) discriminators, which were set for ~ 9 MeV thresholds. The end crystals of each row were excluded in order to reduce the number of events with significant leakage of the electromagnetic shower from the detector. The data trigger required a coincidence between the beam telescope and three or more separated rows of NaI crystals, with no signal in the scintillation counter array. The separation of the crystal rows was enforced by an electronic module that required at least one empty row between rows with signals. If adjacent rows had signals, they were treated logically as one row. After this first level of fast electronics, a second level required that the struck rows of NaI be separated by at least two rows and that the individual NaI crystals responsible for the trigger be separated by two columns (in any single quadrant). The requirement that the triggering crystals be well separated greatly reduced triggers caused by a $\pi^0 \to 2\gamma$ decay in which the electromagnetic shower from one of the photons spread among the crystals in such a way as to strike more than one row. The second-level electronics also required the pattern of rows to be consistent with a momentum-conserving $\pi^0 \to 3\gamma$ event. Because of the relatively large size of the target and the unknown direction of the π^0 recoil, no further use of momentum conservation was feasible in the data analysis.

The time and pulse height in each crystal were recorded for off-line analysis of accepted events. The pulse height was measured by two parallel analog-to-digital converter (ADC) systems having different length gates. The relative response of the two ADC's permitted the identification of individual crystals having a significant amount of energy deposited by an uncorrelated particle ("pileup"). The energy calibration of each crystal was based on the 129.4-MeV radiative-capture photon; a nonlinearity correction ensured that the calibration constants were accurate at lower energies. The resulting calibration[22] was accurate to 0.2 MeV over the entire range of interest, as was verified by measuring the spectrum of 4.4-MeV gamma rays from a Pu-Be source and the single-photon spectrum (55–83 MeV) from $\pi^0 \to 2\gamma$ decays. The time calibration of each crystal with respect to S_1 was based on data from $\pi^0 \to 2\gamma$ decays. Corrections for the energy dependence of the timing and of the time resolution, which were needed for crystal energies below 25 MeV, were obtained from a comparison of the time of a crystal with that of the corresponding scintillator, using $e^{\pm}$'s from $\pi^0 \to \gamma e^+ e^-$. A light-flasher system[26] supplied standard pulses to the crystals during data runs to track drifts in the calibration constants between calibration runs.

III. DATA ANALYSIS

A. Three-photon data

The electromagnetic shower from an interacting photon (or electron) typically spread through several NaI crystals. The first task of the off-line analysis was to identify the crystals associated with a single interaction and then to estimate values for the time, energy, and interaction point of the photon.[25] The highest-energy crystal in the detector was found and the surrounding 5×5 array of crystals was summed to give the energy E_1 of this "clump," excluding crystals with measured times more than 5 ns from that of the central crystals. The process was then repeated for clumps 2, 3, . . . in descending order of energy until all crystals having an energy above 12 MeV were exhausted. (The size of the clump was modified appropriately near the edges or corners of the detector.) If the ADC's indicated that a crystal was piled-up, either the crystal or the whole clump was eliminated, depending upon the energy involved.[25] Figure 3(a) shows the total energy spectrum for $\pi^0 \to 2\gamma$ events in a typical run, as well as a Monte Carlo simulation of the spectrum. The slightly larger full width at half maximum of the data compared to the simulation is caused by small variations in the calibration constants over the course of the experiment.

Clumps were assigned a time by taking a weighted average of the individual crystal times. Figure 3(b) shows the 2γ relative timing spectrum from a typical data run; the resolution is 0.4 ns rms per photon. A position coordinate for each clump was obtained from an energy-

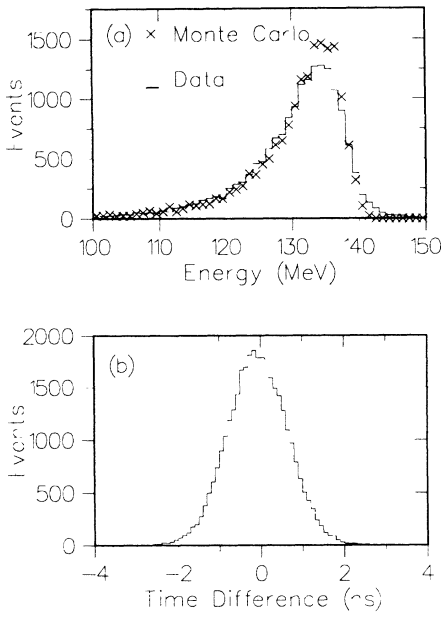

FIG. 3. (a) Total energy spectrum for $\pi^0 \rightarrow 2\gamma$ events, with Monte Carlo simulation; (b) time-difference distribution for $\pi^0 \rightarrow 2\gamma$ events.

weighted average of the centers of the contributing crystal faces. Studies[23] with electrons showed the position resolution to be 1.8 cm rms in both transverse directions on the crystal face.

The recorded events were predominantly of two types: (1) random coincidences of a $\pi^0 \rightarrow 2\gamma$ with another particle; (2) $\pi^0 \rightarrow 2\gamma$ decays that produced three clumps when a secondary photon from one of the initial γ showers interacted far enough from the primary clump to appear as a third clump (referred to as a "split-photon" event). Software cuts on the times and pulse heights of all three beam counters eliminated events caused by multiple incident pions that evaded the hardware rejection based on the S_2 pulse height.

Figure 4 shows the spectrum of the total energy E_T for events that had exactly three neutral clumps with rms time difference less than 4 ns and each clump energy greater than 16 MeV. The time difference between the two highest-energy clumps in these events [Fig. 5(a)] has the expected shape for a prompt coincidence, while that between the two lowest-energy clumps [Fig. 5(b)] shows a peak offset from zero and with two broad shoulders.

The events with $E_T > 142.5$ MeV are found to contribute to the shoulders in Fig. 5(b) centered at $+2$ ns and -3 ns. The two highest-energy clumps in these events have the total energy spectrum and angular distribution expected from a $\pi^0 \rightarrow 2\gamma$ decay. The low-energy clump has a spectrum peaked at the lowest allowed energy (16 MeV) and occurs predominantly in the upstream columns of crystals. Consequently, these events must have been caused by a random coincidence between a π^0 produced in the target and a particle synchronized with the LAMPF 5-ns beam microstructure but originating elsewhere, presumably in some upstream interaction of the beam pions or electrons. These random events can be largely eliminated by two energy cuts: Increasing the minimum clump energy greatly reduces the low-energy photon rate. Rejecting events with $E_T > 142.5$ MeV then eliminates all random events except a few that lie below this cut due to the low-energy tail of the energy resolution function.

Events with $E_T < 142.5$ MeV have a total energy spectrum consistent with the energy response of the detector for 137.8 MeV, the total energy of a π^0. The energy spectra of the highest-energy clump and of the sum of the two lowest-energy clumps both correspond to the $\pi^0 \rightarrow 2\gamma$ single-photon spectrum. Furthermore, the two low-energy clumps tend to be located close together, with E_3 being peaked at the low-energy cut, while the high-energy clump is located nearly opposite the intermediate-energy clump. Hence these events come primarily from a π^0 with a single "split" photon. The shift from zero of the peak in Fig. 5(b) is due to the additional time required for the secondary photon to travel to a distant crystal before interacting. The correlation between the time shift and the distance between clumps is shown

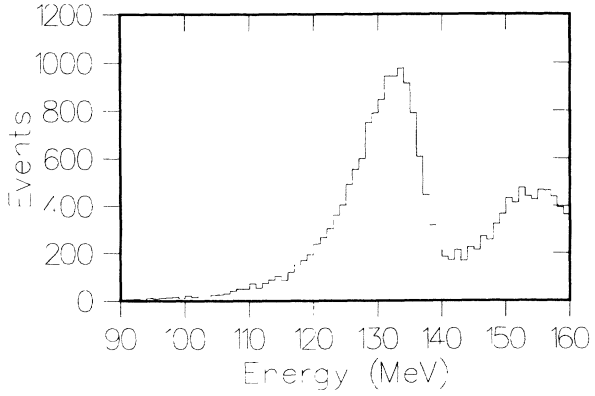

FIG. 4. Total energy spectrum for three-clump events, after cuts as described in text.

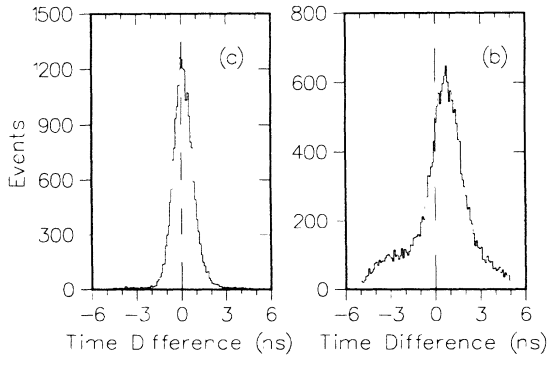

FIG. 5. Time-difference distribution in three-clump events for (a) the two highest- and (b) the two lowest-energy photons.

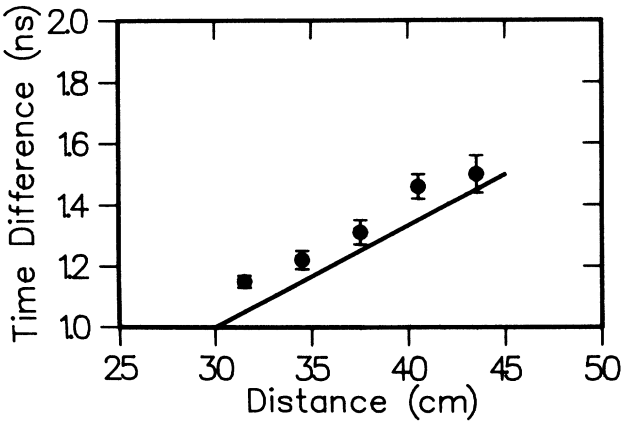

FIG. 6. Average time difference of the two lowest-energy clumps vs their separation distance, for three-clump events. The solid line corresponds to propagation at the speed of light.

in Fig. 6, where the straight line represents travel at the velocity of light. The slopes agree very well. The small offset of the intercepts is attributed to the extra path length of backscattered photons, which were produced after the primary photon penetrated a distance into its crystal and which then reversed this path and entered the face of another crystal.

Split-photon events can be eliminated from the data by increasing both the minimum clump energy and the minimum distance D_{23} between the two lowest-energy photons, while making a tight cut on the relative timing. As a timing criterion, a variable $\chi_t^2 = \sum (t_i - t_m)^2/\sigma_i^2$ was defined, where σ_i is the energy-dependent uncertainty in the time t_i of each clump and t_m is the mean of these times. This statistic is expected to have a χ^2 distribution with two degrees of freedom.

Column N_A of Table I shows the number of events as a function of a cut $E_{\min}$ on the energy of each clump after the following restrictions were placed on the events: $100 < E_T < 142.5$ MeV, $\chi_t^2 < 3$, the minimum separation between each pair of clumps $D_{ij} > 40$ cm, and the angle between the two highest-energy clumps $\theta_{12} < 145°$. Column N_B gives the number of events in the tail of the random-event spectrum extending below 142.5 MeV. This number was estimated by using the known energy resolution function to extrapolate below 142.5 MeV from the distribution of events above that energy, none of which can be split-photon events or real $\pi^0 \to 3\gamma$ events. Column N_U gives a 90%-C.L. upper limit on the net number of $\pi^0 \to 3\gamma$ events remaining in the sample after the subtraction of randoms. We have used a Bayesian calculation[28,29] that assumes a constant prior distribution and that includes the constraint that the net number cannot be negative. For the first two rows a Gaussian approximation is adequate. For the next two rows we have used the Poisson-based algorithm given by Prosper;[29] his factor η is the denominator of the fractions shown. In the final two rows $N_A = 0$, so the limit is based on the usual Poisson algorithm.

TABLE I. Upper limit on the number of 3γ events, N_U, as a function of the cut $E_{\min}$ on the clump energy. N_A and N_B are the number of signal and background events, and ϵ_D is the detection efficiency.

$E_{\min}$	N_A	N_B	N_U	ϵ_D	N_U/ϵ_D
25	10	6.3	8.8	0.012	733
27	5	4.3	5.1	0.010	510
29	3	6/1.83[a]	4.5	0.0089	506
31	2	4/1.96[a]	3.5	0.0069	507
33	0		2.3	0.0050	460
35	0		2.3	0.0032	718

[a]The denominator gives the normalization factor η required in Ref. 29.

Column ϵ_D in Table I gives a Monte Carlo calculation of the detection efficiency for $\pi^0 \to 3\gamma$ events that satisfy these criteria. The matrix element used to generate $\pi^0 \to 3\gamma$ events was that given by Berends.[9] The EGS3 shower simulation code[30] was used to trace photons and electrons through the material between the production point in the hydrogen and the NaI crystal and then to simulate showers in the crystals. Any interaction that would produce a signal in the scintillators and veto the event was automatically taken into account. Monte Carlo–generated signals in the detector were analyzed by the same software used for the off-line data analysis.

The final column in Table I gives the normalized upper limit N_U/ϵ. The decrease in background as $E_{\min}$ increases is roughly balanced by a decrease in detection efficiency, so that N_U/ϵ is insensitive to the value of this cut. Adopting $E_{\min} = 29$ MeV as a reasonable value, the corresponding value of $N_U/\epsilon = 506$.

The above straightforward analysis shows no indication of any $\pi^0 \to 3\gamma$ events in this data. We have also analyzed the data using the maximum-likelihood method, which has the advantage of using the known shapes and correlations of the data distributions instead of simply making cuts on the distributions. Each event was described by a vector $\mathbf{x}$ whose components were: χ_t^2, E_T, the separation distance D between the two closest clumps, and the largest angle between clumps θ_L. The probabilities P, Q, and R that each event in the data sample was a 3γ event, a split-photon event, or a random-photon event, respectively, were calculated from

$$P(\mathbf{x}) = P_1(E_T) P_2(D, \theta_L) P_3(\chi_t^2) ,$$

$$Q(\mathbf{x}) = Q_1(E_T) Q_2(D, \chi_t^2) Q_3(\theta_L) ,$$

$$R(\mathbf{x}) = R_1(E_T) R_2(D) R_3(\theta_L) R_4(\chi_t^2) .$$

Correlated distributions are indicated by the notation.

The individual probabilities P_i, Q_i, and R_i were obtained from the data and from Monte Carlo calculations. To accurately reproduce small energy-calibration shifts during the experiment as well as to allow for the possibility of a slight broadening of the spectrum of three-body events, P_1 and Q_1 were taken from the energy spectrum of the split π^0 events after subtracting the random-photon contribution, rather than from a calibration spectrum. P_2 was obtained from the Monte Carlo calculation and P_3 was calculated from the measured time resolution.

The random-photon probabilities, with the exception of R_4, were obtained from data having one photon arriving early by more than 2 ns. R_4 was taken from events that had three-clump energy sums above 150 MeV.

To determine Q_2 and Q_3, cuts that were uncorrelated with D and θ_L were relaxed to increase the amount of background relative to possible real 3γ data, and the random-photon background was subtracted. The distribution of D was used to generate $Q_2(D,\chi_t^2)$ by simulating the split-photon process, including the 0.1 ns offset shown in Fig. 6. For the secondary photon, $\sigma=0.6$ ns was used for the time resolution in χ_t^2; this value accounted for the increase in σ for photon energies below 20 MeV and for the uncertainty in the distance D.

The likelihood function for N_0 events was defined by

$$L=\prod_{i=1}^{N_0}[N_3P(\mathbf{x}_i)+N_SQ(\mathbf{x}_i)+(N_0-N_3-N_S)R(\mathbf{x}_i)]/N_0 ,$$

where N_3 and N_S are the number of 3γ and split-photon events. The events used in the likelihood analysis were required to have exactly three clumps with a minimum energy of 25 MeV each. The central crystal of each clump was required to have at least 15 MeV to suppress events with poor time resolution. In addition the following cuts were made: $D>25$ cm, $100<E_T<150$ MeV, $\chi_t^2<10$. Figure 7 shows the distributions of D, E_T, χ_t^2, and θ_L for the $N_0=3786$ events remaining in the sample.

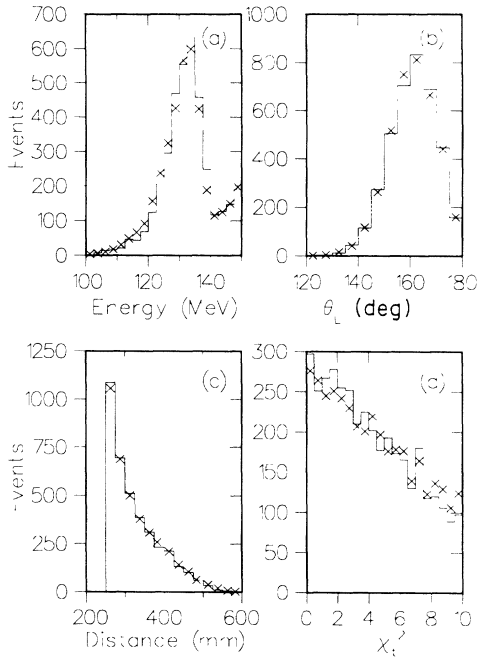

FIG. 7. Histograms of three-clump data used in the likelihood calculation: (a) total energy E_T; (b) largest angle between clumps, θ_L; (c) distance between the two lowest-energy clumps, D; (d) χ_t^2. The $\times$'s are the distributions reconstructed from the maximum-likelihood solution.

The likelihood function L for these events as a function of N_3 and N_S is shown in Fig. 8. L has a maximum at $N_3=1$ (and $N_S=3069$). The projection of L in Fig. 9 was used to obtain an upper limit on the number of $\pi^0\to 3\gamma$ events in the data sample. Defining[29] N_U as the value of N_3 such that 90% of the positive area is between 0 and N_U, one finds $N_U=17$ (90% C.L.).

Introducing Monte Carlo 3γ events into the data sample verified that the likelihood analysis had the appropriate sensitivity to 3γ events. Modifying the background distributions showed that the analysis was not overly sensitive to the exact shape of the distributions. Possible forms for the $\pi^0\to 3\gamma$ matrix element are constrained[9] by angular-momentum conservation, Bose-Einstein statistics, and phase space. Various arbitrary changes in the matrix element produced little change in N_U/ϵ_D. For example, changing to a phase-space distribution changed N_U/ϵ_D by only 2%, because a small decrease in detection efficiency was compensated by a decrease in N_U due to a somewhat greater distinction between 3γ and split-photon events. The detection efficiency itself showed little sensitivity to the matrix element, owing to the smearing of laboratory momenta by the π^0 recoil. Distributions of E_T, D, χ_t^2, and θ_L reconstructed using the likelihood solution are shown with the data distributions in Fig. 7. To compare the reconstruction c_i with the data d_i in each bin i we form $X^2=\sum(d_i-c_i)^2/(\sigma_{d_i}^2+\sigma_{c_i}^2)$, where the σ's are the corresponding statistical errors. The sum over 63 bins yields $X^2=61.9$, indicating satisfactory agreement.

The detection efficiency for 3γ events under the conditions of the likelihood analysis was $\epsilon_D=0.050$, giving $N_U/\epsilon_D=340$. This value is consistent with the values in Table I, but is the result of a more sensitive analysis. The number of observed events N is related to $b_{3\gamma}$ via

$$N=b_{3\gamma}N_{\pi^0}\epsilon_D f_L f_P f_B . \quad (1)$$

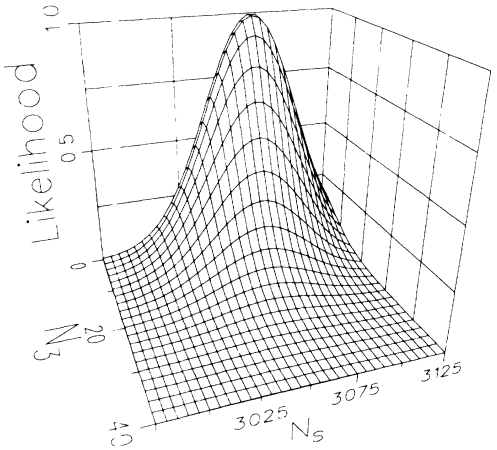

FIG. 8. Likelihood function for selected three-clump events as a function of the number of 3γ events N_3 and the number of split-photon events N_S.

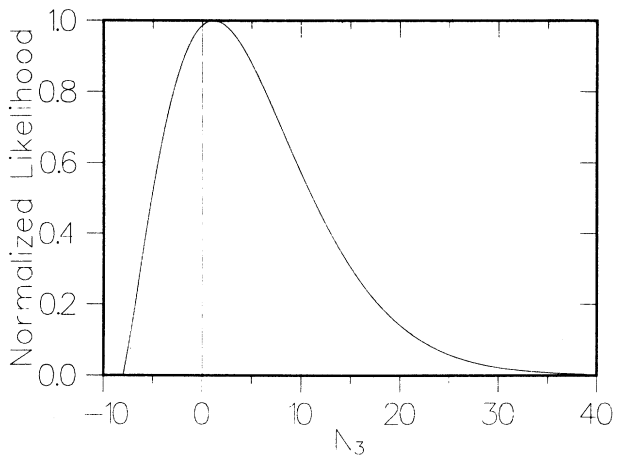

FIG. 9. Projection of the likelihood function in Fig. 8 onto the N_3 axis. The continuation of the function to unphysical negative values of N_3 is shown for reference.

The correction factors are live time $f_L = 0.89 \pm 0.01$, pile-up rejection and accidental-veto factor $f_P = 0.89 \pm 0.02$, and beam-counter cut efficiency $f_B = 0.79 \pm 0.03$. Using $N_U/\epsilon_D = 340$, the upper limit on the 3γ branching ratio is $b_{3\gamma} = 3.1 \times 10^{-8}$ (90% C.L.).

As a check of the overall normalization and systematic errors, the number of $\pi^0 \to \gamma e^+ e^-$ events observed in special charged-trigger runs was compared to a calculated value and found to be $\sim 20\%$ low. Energy loss and multiple scattering of the electrons and positrons make the detection efficiency for these events very sensitive to the details of the sharply peaked angular distributions[31] and of the detector response. We believe that the 2γ monitor is a much more reliable measure of N_{π^0}, but we adopt the 20% discrepancy as a conservative estimate of the overall systematic error in the 3γ branching-ratio limit (and in the 4γ limit in the next subsection). Other sources of systematic error are insignificant in comparison.

B. Four-photon data

The trigger did not reject events in which more than three rows of NaI crystals were struck, so it is possible to search the data for evidence of the decay $\pi^0 \to 4\gamma$. Figures 10(a) and 10(b) show the total energy and χ_t^2 distributions after selecting events with four valid neutral clumps having rms time difference less than 4 ns and E_T between 90 and 160 MeV. No requirement was placed on the clump energies beyond that implied by the energy of the central crystal being greater than 12 MeV. The minimum distance D_{ij} between any two clumps was required to be greater than 20 cm.

The number of candidate events is much smaller than in the 3γ case and Fig. 10(a) shows that relatively few are random events ($E_T > 140$ MeV). Most of the events originate from the splitting of both photons from a π^0. Each of the two lowest-energy clusters tends to be located near one of the two highest-energy ones, and the energies E_3 and E_4 are sharply peaked at the low-energy cutoff. Reducing the number of both random and split photons by raising the minimum clump energy to 15 MeV results in the distributions shown in Figs. 10(c) and 10(d). There is a set of events with small χ_t^2 and $E_T \approx E_{\pi^0}$, but these occur primarily when the low-energy clumps are located near the high-energy ones. These events are consistent with being doubly split π^0 events in which both secondary photons traveled only a short distance, producing little time shift. To eliminate these events, the distances D_{14} and D_{23} were required to be greater than 22.5 cm, and the sum of the energies of the two highest-energy clumps was required to be less than 100 MeV, since a doubly split π^0 would tend to have two clumps whose energy sum approximated the π^0 energy. Figures 10(e) and 10(f) show the result of these cuts: only a few events remain, all having $\chi_t^2 > 9$, whereas 97% of the real 4γ events should lie below 9.

There is therefore no evidence for any $\pi^0 \to 4\gamma$ decays in our data. The 4γ branching-ratio upper limit is calculated from Eq. (1) using $N_U = 2.3$. A Monte Carlo calculation of the detection efficiency using a phase-space distribution gives $\epsilon_D = 0.010$ for the cuts of Fig. 10(f). The other factors are the same as in the 3γ case, except $f_B = 1.0$ because severe cuts on the beam counters were not required to suppress a multiple-pion background. The upper limit $b_{4\gamma} = 2 \times 10^{-8}$ (90% C.L.).

IV. SUMMARY

We have found no evidence for the existence of the C-noninvariant decay $\pi^0 \to 3\gamma$ and set an upper limit on the branching ratio of 3.1×10^{-8} (90% C.L.). This result is an order of magnitude lower than the previous experimental limit and approaches the lower end of the range of theoretical estimates of values that might occur if C invariance did not inhibit the reaction. We have also found no evidence for the C-invariant decay $\pi^0 \to 4\gamma$, setting an upper limit on the branching ratio of 2×10^{-8} (90% C.L.).

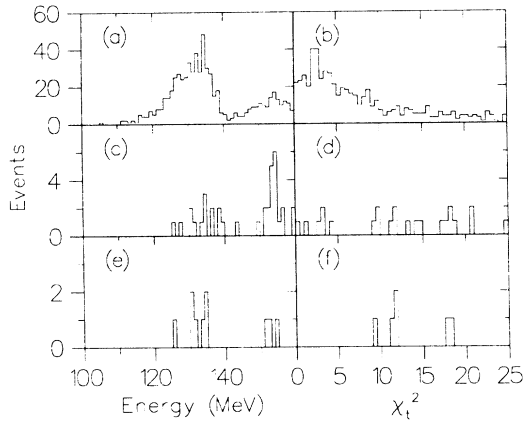

FIG. 10. Total energy [(a),(c),(e)] and χ_t^2 [(b),(d),(f)] distributions of four-clump events. The three sections of the figure show the effect of increasingly restrictive cuts, as described in the text.

ACKNOWLEDGMENTS

We are deeply indebted to many colleagues who helped develop the Crystal Box apparatus over a period of years. We are also grateful for the support given by the LAMPF staff, in particular for that of the hydrogen target group. Finally, we thank Idan Paiss for his help in this experiment. This work was supported in part by the U.S. Department of Energy and the National Science Foundation.

---

*Present address: Department of Physics, Yale University, New Haven, CT 06511.

†Present address: Brookhaven National Laboratory, Upton, NY 11973.

‡Present address: Physics Department, Princeton University, Princeton, NJ 08544.

§Present address: Elektrowatt Ing. AG., Zurich, Switzerland.

**Present address: Physics Department, Virginia Polytechnic Institute, Blacksburg, VA 24061.

††Present address: Swiss Institute for Nuclear Research, CH-5234 Villigen, Switzerland.

‡‡Present address: Argonne National Laboratory, Argonne, IL 60439.

[1]L. Wolfenstein and D. G. Ravenhall, Phys. Rev. **88**, 279 (1952); see references cited therein for related work.

[2]S. DeBenedetti and H. C. Corben, Annu. Rev. Nucl. Sci. **4**, 191 (1954). For more recent work on C invariance in positronium decays, see A. P. Mills and S. Berko, Phys. Rev. Lett. **18**, 420 (1967); and K. Marko and A. Rich, *ibid.* **33**, 980 (1974).

[3]R. P. Ely and D. H. Frisch, Phys. Rev. Lett. **3**, 565 (1959).

[4]T. D. Lee and C. N. Yang, Phys. Rev. **104**, 254 (1956); C. S. Wu, E. Ambler, R. W. Hayward, D. D. Hoppes, and R. P. Hudson, *ibid.* **105**, 1413 (1957); R. L. Garwin, L. M. Lederman, and M. Weinrich, *ibid.* **105**, 1415 (1957).

[5]J. Bernstein and L. Michel, Phys. Rev. **118**, 871 (1960).

[6]D. Cline and R. M. Dowd, Phys. Rev. Lett. **14**, 530 (1965).

[7]J. H. Christenson, J. W. Cronin, V. L. Fitch, and R. Turlay, Phys. Rev. Lett. **13**, 138 (1964).

[8]J. Bernstein, G. Feinberg, and T. D. Lee, Phys. Rev. **139B**, 1650 (1965). See also J. Prentki and M. Veltman, Phys. Lett. **15**, 88 (1965), with an estimate $b_{3\gamma} \sim 10^{-3}$; S. Barshay, *ibid.* **17**, 78 (1965); T. D. Lee, Phys. Rev. **140B**, 967 (1965).

[9]F. A. Berends, Phys. Lett. **16**, 178 (1965).

[10]H. L. Weisberg, University of California Report No. UCRL-16801, 1966 (unpublished).

[11]L. Galfi and G. Marx, Acta. Phys. **22**, 99 (1967).

[12]A. V. Tarasov, Yad. Fiz. **5**, 626 (1967) [Sov. J. Nucl. Phys. **5**, 445 (1967)].

[13]For current knowledge of η asymmetries and references to earlier work, see M. R. Jane *et al.*, Phys. Lett. **48B**, 260 (1974); **48B**, 265 (1974); J. G. Layter, J. A. Appel, A. Kotlewski, W. Lee, S. Stein, and J. J. Thaler, Phys. Rev. Lett. **29**, 316 (1972); J. J. Thaler *et al.*, *ibid.* **29**, 313 (1972). For $\eta \rightarrow 3\gamma$ decay, see D. Alde *et al.*, Z. Phys. C **25**, 225 (1984).

[14]J. Duclos, D. Freytag, K. Schlüpmann, V. Soergel, J. Heintze, and H. Rieseberg, Phys. Lett. **19**, 253 (1965); V. M. Kut'in, V. I. Petrukhin, and Yu. D. Prokoshkin, Pis'ma Zh. Eksp. Teor. Fiz. **2**, 387 (1965) [JETP Lett. **2**, 243 (1965)].

[15]L. B. Auerbach, V. L. Highland, K. F. Johnson, W. K. McFarlane, R. J. Macek, and J. C. Pratt, Phys. Rev. Lett. **41**, 275 (1978).

[16]V. L. Highland *et al.*, Phys. Rev. Lett. **44**, 628 (1980).

[17]S. Weinberg, Rev. Mod. Phys. **52**, 515 (1980); A. Salam, *ibid.* **52**, 525 (1980); S. L. Glashow, *ibid.* **52**, 539 (1980).

[18]A. Soni, University of California at Los Angeles Report No. UCLA/87/TEP/30, 1987 (unpublished), estimated $b_{3\gamma} \sim 10^{-15}$ in the standard model; D. A. Dicus, Phys. Rev. D **12**, 2133 (1975), estimated $b_{3\gamma} \sim 10^{-31}$ from the C noninvariance of the weak interaction.

[19]V. N. Bolotov *et al.*, Pis'ma Zh. Eksp. Teor. Fiz. **43**, 405 (1986) [JETP Lett. **43**, 520 (1986)]; see also L. B. Auerbach, N. Haik, V. L. Highland, W. K. McFarlane, R. J. Macek, J. C. Pratt, J. Sarracino, and R. D. Werbeck, Phys. Lett. **90B**, 317 (1980).

[20]R. L. Schult and B. L. Young, Phys. Rev. D **6**, 1988 (1972).

[21]J. Spuller *et al.*, Phys. Lett. **67B**, 479 (1977).

[22]J. McDonough, Ph.D. thesis, Temple University, 1987; Los Alamos National Laboratory Report No. LA-11056-T, 1987 (unpublished).

[23]R. D. Bolton *et al.*, Phys. Rev. D **38**, 2077 (1988).

[24]S. L. Wilson *et al.*, Nucl. Instrum. Methods **A264**, 263 (1988).

[25]S. L. Wilson, Ph.D. thesis, Stanford University, 1985; Los Alamos National Laboratory Report No. LA-10471-T, 1985 (unpublished).

[26]D. P. Grosnick, Ph.D. thesis, University of Chicago, 1986; Los Alamos National Laboratory Report No. LA-10937-T, 1986 (unpublished).

[27]R. D. Bolton *et al.*, Phys. Rev. Lett. **53**, 1415 (1984).

[28]W. T. Eadie, D. Drijard, F. E. James, M. Roos, and B. Sadoulet, *Statistical Methods in Experimental Physics* (American Elsevier, New York, 1971), pp. 213–214; S. L. Meyer, *Data Analysis for Scientists and Engineers* (Wiley, New York, 1975), pp. 330–331. L. Lyons, *Statistics for Nuclear and Particle Physics* (Cambridge University Press, Cambridge, England, 1986), p. 79.

[29]H. B. Prosper, Nucl. Instrum. Methods **A241**, 236 (1985).

[30]R. L. Ford and R. W. Nelson, Stanford Linear Accelerator Report No. SLAC 210, 1978 (unpublished).

[31]N. M. Kroll and W. Wada, Phys. Rev. **98**, 1355 (1955).